EUROFUSION WPDTT2-PR(16) 16306

P Chmielewski et al.

TECXY simulations of divertor power spreading by impurities seeding in DEMO

Preprint of Paper to be submitted for publication in
Plasma Physics and Controlled Fusion

This work has been carried out within the framework of the EUROfusion Consortium and has received funding from the Euratom research and training programme 2014-2018 under grant agreement No 633053. The views and opinions expressed herein do not necessarily reflect those of the European Commission.

TECXY simulations of divertor power spreading by impurities seeding in DEMO

P. Chmielewski[1], G. Peka[1], I. Ivanova-Stanik[1], R. Zagrski[1], V. Pericol[1,2]

[1] Institute of Plasma Physics and Laser Microfusion, Hery Street 23, 01-497 Warsaw, Poland

[2] ENEA-Frascati, Italy

E-mail: piotr.chmielewski@ifpilm.pl

20 June 2016

Abstract. This paper focuses on numerical studies of the influence of various impurities on edge plasma parameters in the scrape off layer (SOL) region of DEMO tokamak with the standard (SD) and snowflake divertor configuration (SF) with use of the TECXY code. In our model plasma transport in the SOL region is described by classical set of transport equations of multispecies plasma derived by Bragiski, in which electrons and ions are treated as a separate fluid. We solve equations of the model numerically with use of two-dimensional TECXY code, which applies coupled iterative and evolutionary numerical methods. Calculations are performed for the European DEMO1 configuration with the aim to assess the effect of different impurities, e.g. lithium, nitrogen and argon puffing, on edge plasma parameters. It has been found that gas puff of lithium impurities is not sufficient to reduce the energy flux to the divertor plate, while nitrogen and argon impurities result in significant decrease of a total energy flux flowing to the divertor plate, to values smaller than 50 MW, what fully satisfies the DEMO divertor technological limitations.

1. Introduction

Reduction of the energy flux that flows to the wall and to the divertor plate has a substantial meaning for life span and working of a reactor tokamak. Maximum heat fluxes reaching the divertor plate is reliant on maximum tolerable surface temperature and performance of the cooling system [1], thus the power delivered to the core plasma must be absorbed and disperse in the SOL region before it reaches wall and divertor. Such reduction of target heat loads might be achieved by impurities, which concentration can be adjusted to the required energy flux reaching a target [2]. Radiation of the impurities in the scrape off layer can effectively lower heat loads and proceeds in three channels: line radiation, ionization losses and recombination radiation [3]. Note, that the recombination radiation is negligible in comparison to the line radiation. Depending on the type of impurity seeding to the SOL the radiation cooling of the edge plasma

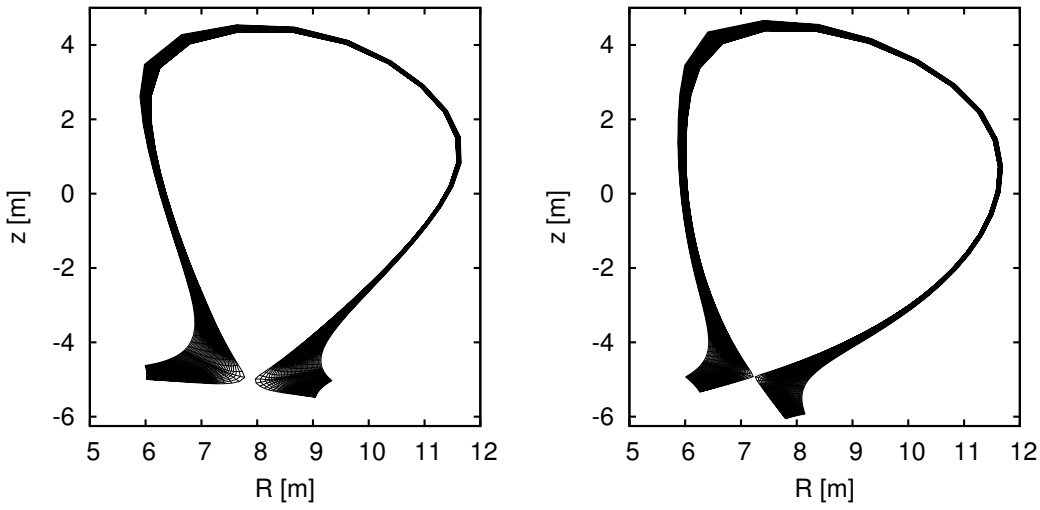

Figure 1. Snowflake (left) and standard divertor (right) numerical mesh configurations.

has a various speed and fraction, which depend on various radiation intensity of specific impurities [4].

To evaluate the influence of the impurity gas puff, there were performed theoretical studies with use of the numerical modelling of the edge plasma in tokamaks [5]. Miettunen et al. [6] with the use of numerical simulations, which apply Monte-Carlo orbit-following code ASCOT, shows that plasma flows drives particles strongly towards the inner divertor and that the beryllium impurity is deposited on the inner tokamak divertor. A temperature and heat flux densities reduction at the low-field side divertors was obtained by Rozhansky et al. [7] for Super-X divertor configuration of the MAST Upgrade tokamak. They used the SOLPS numerical code with included a magnetic gradient and an electric field drifts effects. Ono el al. [8] analyzed and well portrayed profiles of heat and particle fluxes reaching divertor plates obtained in the NSTX experiment with use a 3-dimentional model of edge transport with coupled plasma fluid and kinetic neutral particles simulations (EMC3-EIRENE).

On the other hand, the amount and types of impurities can be dependent on the divertor plate material, which diffuse to the edge plasma in process of sputtering and increase the impurity radiation in the SOL/core regions [9].

The paper is organized as follows. The numerical model and investigated problems are presented in Sec. 2. Description and discussion of results are contained in Sec. 3, while the summary and conclusions of our studies are placed in Sec. 4.

2. Numerical simulations

Our model of a plasma transport in the SOL region is described by classical set of transport equations of multispecies plasma derived by Bragiski [10], in which electrons

and ions are treated as a separate fluid. The plasma and impurity transport is classical along the magnetic field lines with transport coefficients derived from 21 moment Grad approximation [11], while transport across the magnetic field lines is anomalous with diffusion coefficients of the order of Bohms diffusion. The temperature of plasma ions and impurity ions temperature is assumed to be the same.

We solve equations of the model numerically with the use of two-dimensional TECXY code, which apply coupled iterative and evolutionary numerical methods [12-13]. However, the TECXY applies a simple analytical description of neutrals distribution as well as it contains divertor plates perpendicular to poloidal component of magnetic field, Rubino et al. [14] shown that the TECXY numerical code reveals a good agreement with results of simulations of SOL plasma in DEMO made with use of EDGE2D/EIRENE code, while Apicella et al. [15] remarked TECXY simulations agreement with experimental data for the edge plasma with impurity gas puffing obtained in the FTU tokamak. We perform a numerical calculations for the DEMO reactor, for which the power flowing through the separatrix is potentially much higher than for experiments done up to now and for the ITER. An allowable limit of the heat flux at the target has been postulated to be below 5 MWm^{-2}, while the divertor plasma temperature should be below 5 eV to satisfy an acceptable erosion limit of the target [16].

In our model the SOL region is covered by the non-uniform numerical mesh, that is denser near divertor plates and the core region, while it is rare in the mid plane region and near the tokamak wall. We consider two types of the divertor configurations: the snowflake (SF) and the standard (SD) divertor configurations, which have separate numerical meshes shown in Fig. 1. The top panel illustrates SF mesh in the $R-Z$ plane of toroidal coordinates, while the bottom panel presents SD mesh. Differences in the spatial distribution of divertors in SF and SD cases, thus differences in the magnetic field line configuration in the SOL, specifically in the region of the null point, is well seen on Fig. 1. Magnetic field lines in the case of SF configuration are much more diverged and the null point affected zone is much larger than in the case of SD configuration, where the last close magnetic surface (LCMS) run close to the null point (Fig. 1., bottom panel).

Numerical studies are performed for three values of the input heat flux, P_{input}, crossing the separatrix: 100 MW, 150 MW and 200 MW, whereas the particle flux of the main plasma across separatrix into the SOL is set to be equal to 2×10^{23} s^{-1}. The anomalous transport of plasma particles across magnetic field lines is described by the particle diffusion coefficient $D = 0.42$ $\mathrm{m}^2\mathrm{s}^-1$ and the energy diffusion coefficient $\chi = 0.179$ $\mathrm{m}^{-1}\mathrm{s}^{-1}$, which are hold fixed. Assumed recycling coefficient for hydrogen frecyc is equal to 0.95, while for impurities fzrecyc is equal to 0.25.

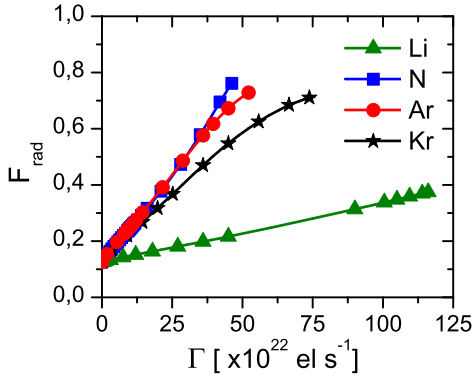

Figure 2. Radiation fraction vs. the gas puff of lithium (triangles), nitrogen (squares), argon (circles) and krypton (stars) impurities for the input power equal to 150 MW in the SD divertor configuration.

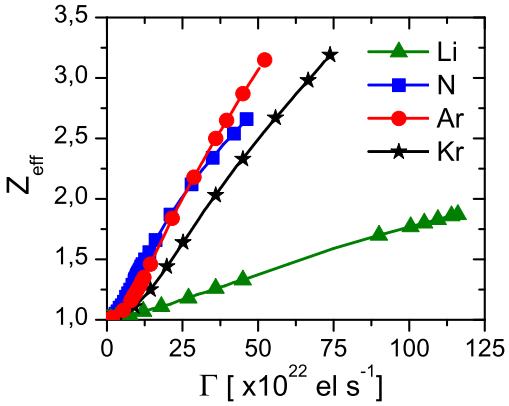

Figure 3. Effective charge change with gas puff of lithium (triangles), nitrogen (squares), argon (circles) and krypton impurities (stars) for case with standard divertor configuration and the input power equal to 150 MW.

3. Results

3.1. Different impurity types

Depending on the type of impurity, which is puffed into the SOL, the plasma properties vary differently. We consider impurity seeding by lithium, nitrogen, argon and krypton atoms separately and compare the obtained results for SD magnetic field configuration. This attitude give us opportunity to examine the influence of puffing of each element to the SOL on the edge plasma parameters.

As we expect, along with growth of impurity flux, puff, the total radiation in the SOL increases. Figure 2 illustrates the radiation fraction, Frad, which is defined as a ratio of the total electron energy losses to the total input heat flux through separatrix,

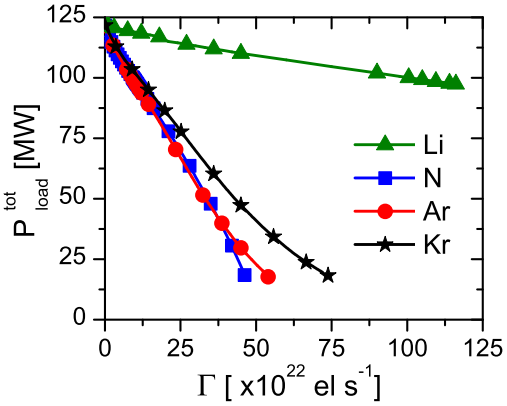

Figure 4. Total power load to the plate vs. the gas puff of lithium (triangles), nitrogen (squares), argon (circles) and krypton (stars) impurities for the input power equal to 150 MW. Here the SD magnetic field line configuration is applied.

Pinput. Frad is almost linearly rising with puff, however comparing different types of impurity, we note faster increase of F_{rad} for argon (Fig. 2, circles) and nitrogen (squares) reaching a value of 0.75, while the slowest for lithium (triangles), where F_{rad} is below 0.4. It should be noticed that krypton impurity with possible thirty six ionization states, radiates less than nitrogen and argon impurities for given impurity flux, Γ_{puff}, as predicted by simple corona cooling rates.

Increase of the flux of impurities leads to decrease of the total power to the divertor plate, P_{PLATE}, and an increase of the effective charge in the SOL region, that we observe on Fig. 3. Here, the fastest growth of the effective charge with a gas puff is observed for argon impurities (red stars), which reach a value about 3.25. As well Z_{eff} of krypton reaches high value, but discernible lower in comparison to the argon impurities gas puff. However, N impurities gas puff leads to increase of Z_{eff} as fast as Ar ions gas puff (full red dots), they get a maximum value of the effective charge below 2.75 (full blue squares).

In Fig. 4, there is presented the fall off of P_{PLATE} with Γ_{puff} for lithium (triangles), nitrogen (squares) argon (circles) and krypton (stars) for $P_{input} = 150$ MW.

As the radiation of energy in the SOL is the most efficient for nitrogen and argon (Fig. 2, squares and stars, respectively) the total power to the target is almost completely mitigated by this type of impurities in contrary to lithium one (triangles). The total power, which reaches divertor surface drops to about < 20 MW in case of N, Ar and Kr seeding. On the other hand, Li ions are not able to reduce energy in the SOL and the power reaching target plate exceeds value of 95 MW, which might quickly damage the divertor of the DEMO tokamak. We report that gas puffing of lithium impurities is not sufficient to reduce the energy flux to the divertor plate, while nitrogen and argon impurities result in significant decrease of energy flux flowing to the divertor plate, to values much smaller than 50 MW. Flux of the total power to the plate at this level fulfil

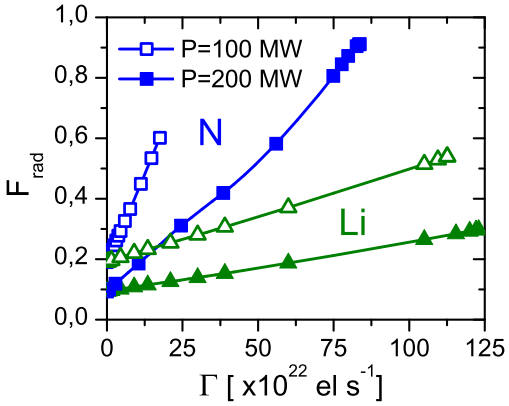

Figure 5. Radiation fraction vs. the gas puff of lithium (triangles) and nitrogen (squares) impurities for the total input power equal to 100 MW (open symbols) and 200 MW (full symbols) in the case of the SD divertor configuration.

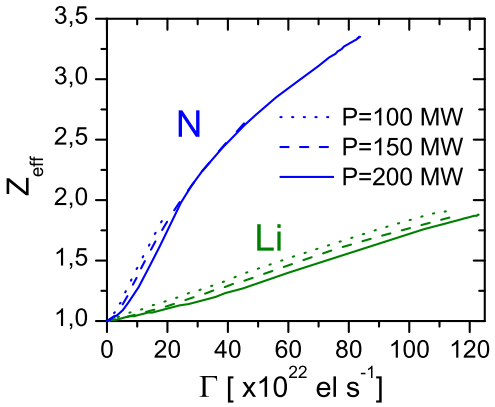

Figure 6. Effective charge vs. gas puff of lithium and nitrogen for case SD configuration and the input power equal to 100 MW (dotted line), 150 MW (dashed line) and 200 MW (solid line).

the DEMO divertor technological limitations [17].

3.2. Input power influence

Changes of radiation fraction with the total power to the plate are shown on the Fig. 5. We notice that increase of the radiation fraction of nitrogen (squares), as well as argon and krypton impurities (not shown), varies considerably for the low values of P_{input} =100 MW (open symbols) and for the high P_{input} =200 MW (full symbols). Seeding impurities under the power 100 MW results in radiation fraction for nitrogen at the level 0.6, (similar values are for argon and krypton). On the contrary, F_{rad} under the input power equal to 200 MW for nitrogen rises up to a value of 0.9. Plasma in the SOL needs higher impurity flux (Γ_N(200 MW) $\simeq 60\times10^{22}$ el s^{-1} in comparison to Γ_N(100 MW) $\simeq 20\times10^{22}$

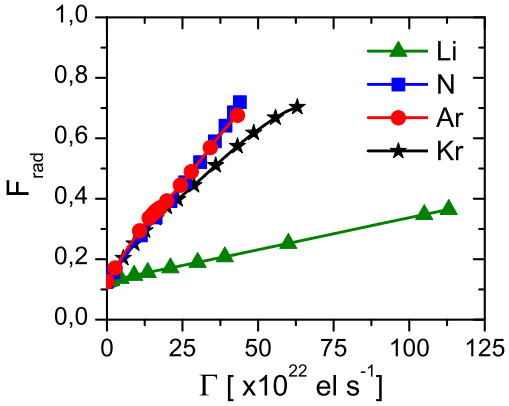

Figure 7. Radiation fraction vs. the gas puff of lithium (triangles), nitrogen (squares), argon (circles) and krypton (stars) impurities for the input power equal to 150 MW in the SF divertor configuration.

el s−1) to radiate at the similar level equal to 0.6 (Fig. 5, full squares and open squares, respectively). Notice, that the radiation efficiency of lithium is rather low and Frad is not able to reach high values. Additionally, due to slower increase of the radiation fraction with Γ_{puff} for P_{input} =200 MW, values of F_{rad} are even lower than for 100 MW. The effective charge growth with the increase of gas puff is shown on Fig. 6 for N and Li impurities. Here, different input powers to the SOL are distinguished by different lines: doted for P_{input} =100 MW, dashed for P_{input} =150 MW and solid for P_{input} =200 MW. The observed quasi-linear growth of the effective charge is a consequence of the increasing concentration of impurities Z_{eff} that reaches higher values for nitrogen (blue solid line) and argon (not shown) than for lithium (green soli line), approaching the value of 3.5 for the nitrogen and less than 2 for lithium under P_{input} = 200 MW. It should be noted that with rising values of the input power and Γ, the impurity ionization, thus effective charge increases, however Zeff for given impurity flux stay at the similar level.

3.3. Comparison of the SF and SD configuration

To be able to make a comparison of two types of magnetic field configurations, we plot the radiation fraction vs. the gas puff of lithium, nitrogen, argon and krypton impurities for the input power equal to 150 MW in the SF divertor configuration (Fig. 7) and collate to analogue Fig. 2. Notice that essentially there is no difference between results obtained for the snowflake and standard divertor configurations. As with the case of SD configuration, F_{rad} increase faster with Γ for argon (circles) and nitrogen (squares) reaching a value of 0.75, while the radiation fraction growth is the slowest for lithium (triangles), where F_{rad} is below value of 0.4. On the other hand, a comparison of the effective charge variation with gas puff, shown at Fig. 8, reveals a higher values of Z_{eff} for SF configuration than for SD under the same gas puff. Observed, small differences between the magnetic field configurations are the evidence of a higher impurity retention

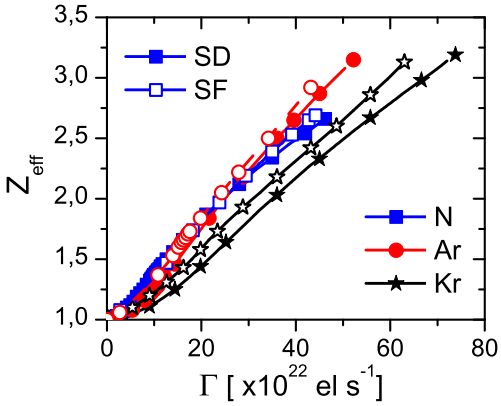

Figure 8. Effective charge change with gas puff of nitrogen (squares), argon (circles) and krypton impurities (stars) for case with SD (full symbols) and SF (open symbols) configuration and the input power equal to 150 MW.

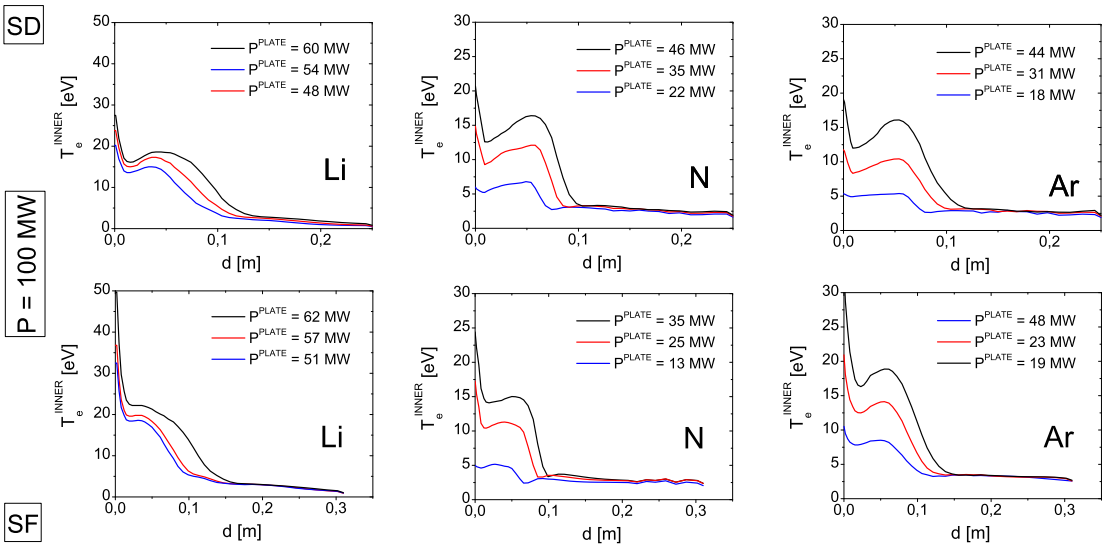

Figure 9. Profiles of the electron temperature at the inner divertor plate in the SF divertor configuration (top) and at the outer divertor plate in the SD divertor configuration (bottom) for the total input heat flux equal to 100 MW. Black solid line corresponds to the low value of the gas puffing, Γ, red line to middle value of gas puffing and blue line to the large value of Γ, in the case of lithium impurity gas puffing (left), nitrogen impurity gas puffing (middle) and argon impurity gas puffing (right) .

in the case of SF.

3.4. Divertor plate analysis

We also perform analysis of the plasma parameters at the divertor plates. On Fig. 9 and Fig. 10, there are shown profiles of the electron temperature at the plate for different

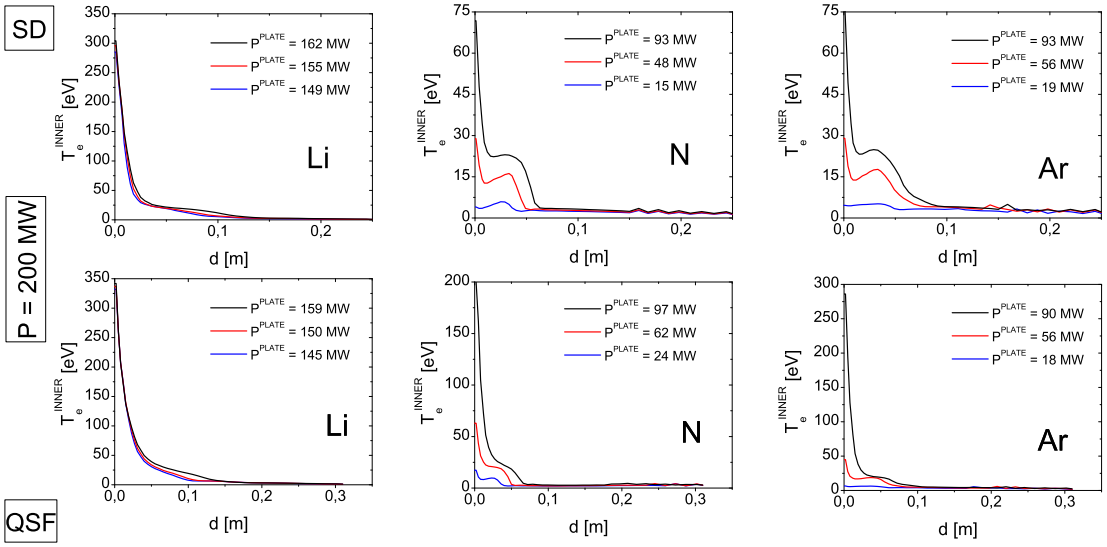

Figure 10. Profiles of the electron temperature at the inner divertor plate in the SF divertor configuration (top) and at the outer divertor plate in the SD divertor configuration (bottom) for the total input heat flux equal to 200 MW. Black solid line corresponds to the low value of the gas puffing, Γ, red line to middle value of Γ and blue line to the large value of Γ, in the case of lithium impurity gas puffing (left), nitrogen impurity gas puffing (middle) and argon impurity gas puffing (right) .

input heat fluxes equal to 100 MW (Fig. 9) and 200 MW (Fig. 10). Black, red and blue lines corresponds to small (black line), average (red line) and large (blue line) impurity influx, respectively. The radial distance from the strike point, d, is presented at $x-$axis. The electron temperature profiles at the divertor plate reach the maximum value near the strike point regardless of the divertor configuration, the input heat flux and the type of the impurity seeding. We recognize non-uniform fall off of the electron temperature, T_e, along the plate. Notice, that in the SF divertor configuration Te has slightly larger values, than in the SD configuration. For instance, in the case of SF (SD) divertor configuration and a middle level of gas puff for N and Ar, Te in the strike point reaches about 20 eV (15 eV) for $P_{input} = 100$ MW and about 50 eV (30 eV) for $P_{input} = 200$ MW.

Next, for the highest puff rate, it drops abruptly from the maximum at the strike point till certain value of the electron temperature at $y \simeq 0.02$ m, which is in the range of 8 eV and 25 eV, in accordance with the P_{input}, type of divertor configuration and value of the impurity flux, then it subtly rises, growing by few eV. Finally, at d =0.1 m the electron temperature starts slowly falling down up to level of few eV.

4. Conclusions

In this work we have performed numerical analysis of the plasma transport in the SOL region for the European DEMO1 configuration in view of various types of impurities, input power as well as magnetic field configuration. It has been found that the gas puffing of lithium impurities is not sufficient to reduce the energy flux to the divertor plate, while nitrogen and argon impurities result in significant decrease of energy flux flowing to the divertor plate, to values smaller than 50 MW, what marginally satisfies the DEMO divertor technological limitations. We came to the conclusion that to prevent a target plate from high energy flux influence the lithium impurity cannot be applied independently, but has to accompanied by seeding of additional impurity with higher atomic number. As shown the radiation fraction reaches larger values in case of nitrogen and argon impurities seeding in comparison to lithium one. It is worth notice, that independently of the impurity type (except of lithium) the local maximum of the temperature profile at the plate suffers shift towards the strike point, while the flux of impurities increases (Figs. 9 and 10, middle and right panels). Additionally, we remark that regardless of the chosen model of the divertor configuration: SD or SF, the impurity radiation of individual elements in the SOL remains at the similar level, however, the impurity retention is better in the case of SF configuration.

5. Acknowledgments

This work has been carried out within the framework of the EUROfusion Consortium and has received funding from the Euratom research and training programme 2014-2018 under grant agreement No 633053. The views and opinions expressed herein do not necessarily reflect those of the European Commission.

References

[1] Herrmann A. 2002 Plasma Phys. Control. Fusion 44 883903
[2] Rapp J. et al. 2004 Nucl. Fusion 44 312319
[3] Morozov D. Kh. et al. 2007 Plasma Phys. Reports 33 11 906922
[4] Ivanova-Stanik I. & Zagrski R. 2015 J. Nucl. Mater. 463 596600
[5] Zagrski R. 1996 J. Tech. Phys. 37 1 7-37
[6] Miettunen J. et al. 2013 J. Nucl. Mater. 438 S612-S615
[7] Rozhansky V. et al. 2013 Nucl. Fusion 50 3 034005
[8] Ono M. et al. 2000 Nucl. Fusion 40 3Y 557
[9] Ivanova-Stanik I. & Zagrski R. 2015 Nucl. Fusion 55 073034 (6pp)
[10] Bragiski S.I. 1965 Rev. Plasma Phys. 1 205
[11] H.A. Claassen et al. 1991 Longitudinal transport coefficients of a magnetized plasma consisting of hydrogen and a single impurity element in arbitrary populated charge state. Technical Report July-2-423 Institute of Plasma Physics, Juelich
[12] Gerhauser H. et al. 2002 Nucl. Fusion 42 805-813
[13] Gerhauser H. et al. 2006 Nucl. Fusion 46 1 149
[14] Rubino G. et al. 2016 Comparative analysis of the SOL plasma in DEMO using EDGE2D/EIRENE and TECXY codes. 22th PSI conference, Roma

[15] Apicella M. L. et al. 2012 Plasma Phys. Control. Fusion 54 3 035001
[16] Zohm H. et al. 2013 Nucl. Fusion 53 7 073019
[17] Wenninger R.P. et al. 2014 Nucl. Fusion 54 11 114003
[18] Gerhauser H. et al. 2002 Nucl. Fusion 42 805-813